2010 AIAA SDM, Wind Energy Session, Orlando, AIAA-2010-2820

Fatigue Trends for Wind Blade Infusion Resins and Fabrics

Daniel D. Samborsky, Pancasatya Agastra and John F. Mandell,
Department of Chemical and Biological Engineering, Montana State University,
Bozeman, MT, 59717, USA

ABSTRACT

This paper presents recently expanded test data for resin infused glass fiber laminates of interest for wind turbine blades. The new static and fatigue data extend and clarify trends reported in References 3-7 for the relative performance of epoxy, vinyl ester and polyester resins, and various unidirectional (UD) and biaxial (±45) fabrics, and multidirectional (MD) combinations, in standard laminate tests. Significant resin, fabric and process interactions are identified and explored. A second part of the study involves characterizing the performance of the various fabrics and resins in the context of a recently developed complex structured coupon geometry including ply drops. This coupon provides a simplified approach to exploring the relative performance of blade materials in the context of the complex structural details typical of infused blades. This testing approach highlights the significance of resin toughness differences in a representation which can conveniently be applied to blade design as strain knockdown factors.

I. Introduction and Background

Recent studies of the fatigue of infused wind turbine blade fiberglass laminates have shown significant effects of fabric construction on the tensile fatigue performance, which is a critical parameter in blade performance [1-7]. The effects of several unidirectional stitched fabrics of generally similar construction and fiber volume percent, V_f, are illustrated for the epoxy resin laminates shown in Figure 1 (fabric, resin and laminate designations are given in the following section). Nearly a factor of two difference in fatigue strains between laminates with different fabrics is shown for the same lifetime in these S-N curves, which represent the maximum (measured) initial strain in the fatigue test vs. cycles to failure, fit with a power law model (Eq. 1) and plotted in a linear strain - log cycles format.

$$S = A\,N^{B} \qquad (1)$$

Where S is the maximum stress or strain in each constant amplitude fatigue cycle, N is the cycles to failure (complete separation), and A and B are constants; the power law is fit to the fatigue data only, unless noted. While the strain is the more general parameter for materials comparisons and many blade design procedures, only the initial strain on the first few cycles can be measured, and subsequent strain increases due to softening are not represented. Stress plots are also given in many cases, but these are sensitive to laminate construction (% 0-degree plies) and fiber content differences when comparing materials. The stress and strain values are not generally proportional, since many stress-strain relationships are nonlinear, particularly for biax fabric laminates.

The tensile fatigue performance can be compared through metric of the (initial) strain which can be withstood for a million cycles (other metrics are discussed later). When a broad range of laminates, fabricated to different fiber contents in vacuum assisted resin transfer molding (VARTM) by controlling the two-sided mold opening, were compared in terms of million cycle strain and fiber volume fraction, the results in Figure 2 have been reported [1,4,7]. The early results for fabric A laminates [3] used polyester resin and a low density fabric shown in Figure 3, which was compressed to high fiber content in the VARTM mold. The other data represent higher density fabrics currently used in resin infused blades, with epoxy resins; these fabrics are shown in Figure 4. The data in Figure 2 show a marked transition in fatigue strain as the fiber content increases. Data for particular laminate groups show a range of transition fiber contents from around 45% to around 60% depending on the particular fabric and resin. Fabrics with very similar weight and construction, like C and D in Figure 4, showed significant differences in fatigue performance [1,4,7].

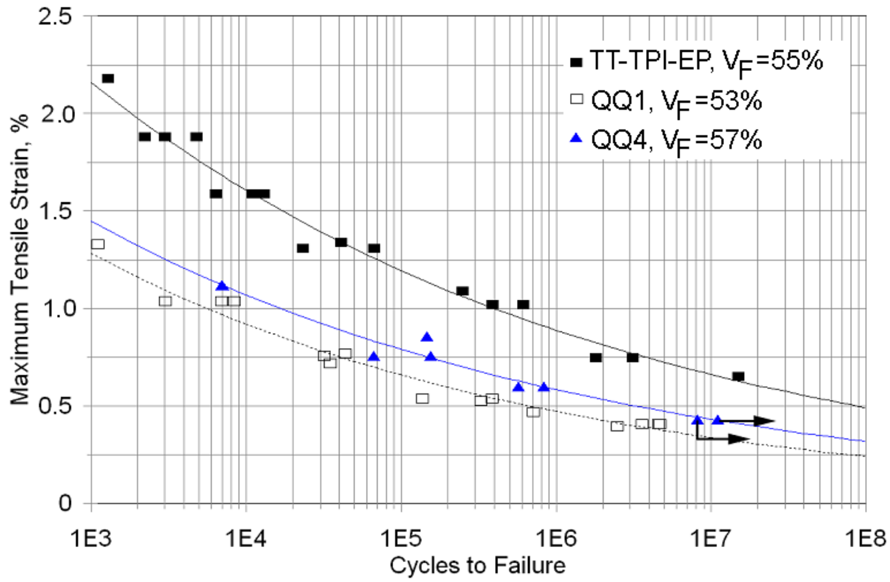

Figure 1. Comparison of tensile fatigue resistance for multidirectional laminates based on unidirectional fabrics B (QQ1), C (QQ4), both VARTM processed, and D (TT-TPI-EP), SCRIMP processed [1].

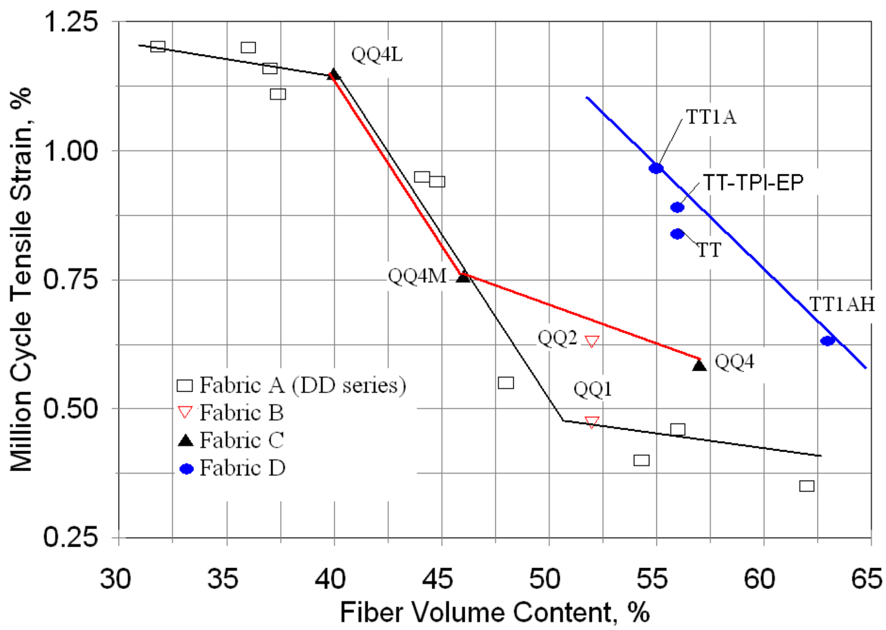

Figure 2. Million cycle strain vs. fiber volume content for various VARTM laminates and one SCRIMP laminate (TT-TPI-EP) showing transitions to reduced fatigue resistance as a function of 0^{o} fabric, R = 0.1 [1].

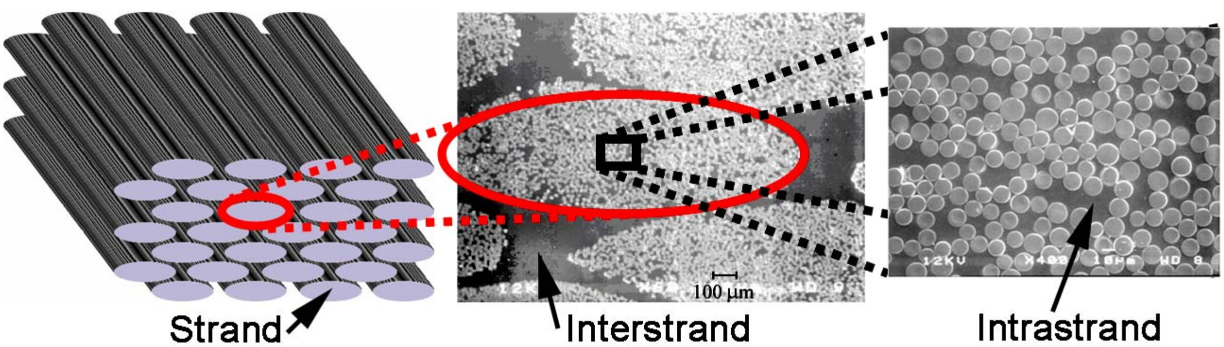

Figure 3. Fabric A (low density) exploded view [1].

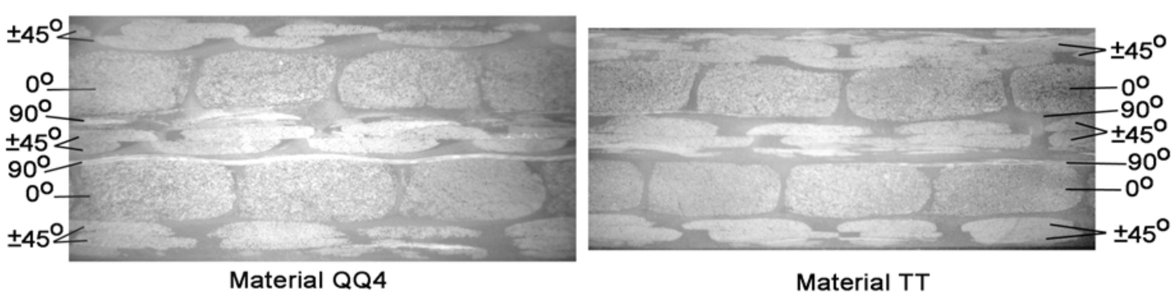

Figure 4. VARTM processed laminates with high density unidirectional fabrics, QQ4 (fabrics C and M), and TT (fabrics D and M) [1].

II. Experimental Methods

A. Materials and Processing

Tables 1, 2 and 3 give details of the resins, fabrics, laminate constructions used in this study. Laminates were processed either by VARTM, Figure 5, or by infusion through resin flow media, Figure 6. SCRIMP processing is a variant of the infusion process, also with a hard mold on one side only. Details of processing can be found in Reference 1.

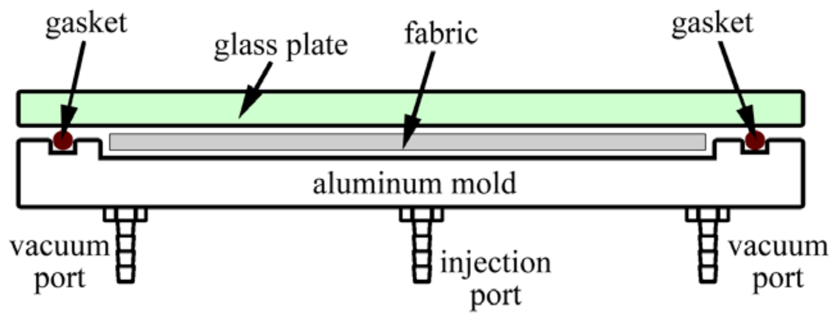

Figure 5. Schematic of the VARTM process, two-sided mold

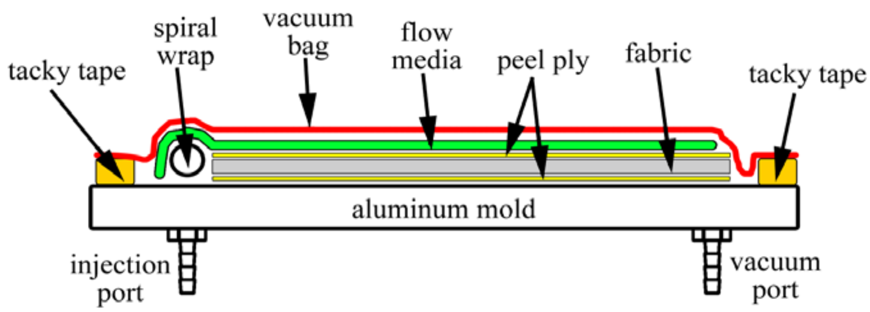

Figure 6. Schematic of the resin infusion process, one-sided mold

Table 1. VARTM/Infusion Resins and Post Cure Conditions

Name	Type	Resin	Cure (if not RT) and Post Cure* Temperature, ^{o}C
EP-1	Epoxy	Hexion MGS RIMR 135/MGS RIMH 1366	80
EP-1a	Epoxy	Hexion MGS RIMR 135/MGS RIMH 1366	35 and 70
EP-2	Epoxy	Huntsman/Vantico TDT 177-155	70
EP-3	Epoxy	SP Systems Prime 20LV	80
EP-4	Epoxy	Huntsman Araldite LY1564/XB3485	60 and 82
EP-5	Epoxy	Hexion MGS L135i/137i	35 and 90
EP-6	Epoxy	Jeffco 1401	60 and 82
EP-7	Epoxy	DOW un-toughened epoxy	90
EP-8	Epoxy	DOW toughened epoxy	90
UP-1	Polyester	U-Pica/Hexion TR-1 with 1.5% MEKP	90
UP-2	Polyester	CoRezyn 63-AX-051 with 1% MEKP	65
UP-3	Polyester	Ashland AROPOL 1101-006 LGT with 1.5% DDM-9 MEKP	65
UP-4	Polyester	CoRezyn 75-AQ-010 with 2.0% MEKP	65
UP-5	Polyester	Reichhold Polylite X4627-31 with 2% MCP-75FRED	25 and 70
VE-1	Vinyl ester	Ashland Derakane Momentum 411 with 0.1% CoNap, 1% MEKP and 0.02 phr 2,4-Pentanedione	100 65 (mixed mode)
VE-2	Vinyl ester	Ashland Derakane 8084 with 0.3% CoNap and 1.5% MEKP	90
VE-3	Vinyl ester	Ashland Derakane 411-200	NA
pDCPD	pDCPD	Materia, Inc.	NA

*Actual temperatures used for test panels; may not comply with manufacturer recommendations for blades.

Table 2. Glass fabric specifications (from manufacturers).*

	Manuf.	Designation	Areal Wt. (g/m^2)	Component Strands* Warp Dir.(wt.%)				
				0^o	$\pm 45^o$	90^o	Mat	Stitch
A	Knytex	D155	527	0	0	99	0	1
B	Saertex	U14EU920-00940-T1300-100000	955	91	0	8	0	1
C	Saertex	S15EU980-01660-T1300-088000	1682	97	0	2	0	1
D	Vectorply	E-LT-5500	1875	92	0	6	0	2
E	Vectorply	E-LM-1810	932	67	0	0	32	1
F	Vectorply	E-LM-3610	1515	80	0	0	20	0
G	Vectorply	E-LM-3900	1346	90	0	9	0	1
H	PPG-Devold LLC	L1200/G50-E07	1261	91	0	4	4	1
L	Saertex	VU-90079-00830-01270-000000	831	0	97	2	0	1
M	Fiber Glass Ind.	SX-1708	720	0	68	0	30	2
N	Vectorply	E-BX-1700	608	0	99	0	0	1
O	OCV	WindStrand DB1000	1000	5	94	0	0	1
P	PPG-Devold LLC	DB810-E05-A	808	0	99	0	0	1

* Historically, component E-glass strands are not identified for most fabrics, and different strands may be substituted for different fabric runs. However, the strands in fabrics D, G, H and P contain PPG Hybon® 2026 sized strands; fabric M contains FGI 675/1334 strands; and fabric O contains OCV WindStrand 17-1200 SE2350M2 strands.

Table 3. Laminate Definition

Database Laminate Designation	Resin	Fabrics	Layup	V_f (%)	Thickness (mm)	Process	Processed by (if not MSU)
Glass, 0^o and ±45^o Plies							
DD series	UP-2	A, K	$(0/\pm45/0)_S$	Var.	Var.	VARTM	
QQ1	EP-2	B, L	$(\pm45/0_2)_S$	53	4.09	VARTM	
QQ1I	EP-1	B,L	$(\pm45/0_2)_S$	52	4.10	infusion	
QQ2	EP-2	B, L	$(\pm45/0/\pm45)_S$	52	3.96	VARTM	
QQ4	EP-2	C, M	(±45/0/±45/0/±45)	57	4.03	VARTM	
QQ4I	EP-1	B, L	$(\pm45/0/\pm45)_S$	50	4.59	infusion	
QQ4-L	EP-2	C, M	(±45/0/±45/0/±45)	40	5.70	VARTM	
QQ4-M	EP-3	C, M	(±45/0/±45/0/±45)	46	4.85	VARTM	
SLA	UP-3	D, N	(±45/0/±45/0/±45)	54	4.29	Scrimp	Vectorply
SLB	UP-3	E,N	(±45/0/±45/0/±45)	43	2.69	Scrimp	Vectorply
SLC	UP-3	F,N	(±45/0/±45/0/±45)	51	3.67	Scrimp	Vectorply
TT-TPI-EP	EP-4	D, M	(±45/0/±45/0/±45)	55	4.59	Scrimp	TPI
TT-TPI-VE	VE-3	D, M	(±45/0/±45/0/±45)	55	4.60	Scrimp	TPI
TT	EP-3	D, M	(±45/0/±45/0/±45)	55	4.60	VARTM	
TT	EP-1	D, M	(±45/0/±45/0/±45)	55	4.60	Scrimp	
TT	UP-1	D, M	(±45/0/±45/0/±45)	52	4.60	Scrimp	
TT2	EP-1	D,M	(±45/0/0/0/±45)	54	6.60	infusion	
TT5	EP-1	H,P	$(\pm45/\pm45/{}_{90}0/0_{90})s$	56	5.73	infusion	
TT5	EP-1a	H,P	$(\pm45/\pm45/{}_{90}0/0_{90})s$	58	5.56	infusion	
TT5	UP-5	H,P	$(\pm45/\pm45/{}_{90}0/0_{90})s$	58	5.55	infusion	
TT7	EP-1	G,M	(±45/0/±45/0/±45)	48	4.23	infusion	
TT1A	EP-2	D, L	(±45/0/±45/0/±45)	55	4.37	VARTM	
TT1A	EP-1	D, L	(±45/0/±45/0/±45)	55	4.37	infusion	
TT1A-H	EP-2	D, L	(±45/0/±45/0/±45)	63	3.98	VARTM	
UDH-EP-1	EP-1	H	$({}_{90}0/0_{90})$	57	1.72	infusion	
UDH-UP-5	UP-5	H	$({}_{90}0/0_{90})$	61	1.60	infusion	
TT1A-pDCPD	pDCPD	D,L	(±45/0/±45/0/±45)	64	4.00	infusion	Materia
±45^o plies only							
DH	EP-1	M	$[(RM/-45/45)s]_3$	44	4.57	infusion	
DTR1	UP-1	M	$[(RM/-45/45)s]_3$	44	4.52	infusion	
45D	VE-1	M	$[(RM/-45/45)s]_3$	46	4.12	infusion	
45D2	VE-2	M	$[(RM/-45/45)s]_3$	44	4.41	infusion	
SWA	EP-1	L	$(\pm45)_{3S}$	45	4.20	infusion	
DE2	EP-7	M	$(\pm45)_{3S}$	40	4.93	infusion	
DE4	EP-8	M	$(\pm45)_{3S}$	40	4.85	infusion	
W45	EP-1	O	$(\pm45)_6$	49	4.10	infusion	

B. Test Methods

Test methods have been described in detail elsewhere [1,3]. Panels were machined to the dog bone shape indicated in Figure 5 for tensile fatigue, loaded in constant amplitude at R = 0.1, load control, sine wave at 1-5 Hz, with forced air cooling to limit surface temperature rise to less than 5°C. Tests are reported for several R-values, where R = minimum load/maximum load; the rectangular specimens in Figure 5, with a 13 mm gage length and 25 mm width, were used for compression and reversed loading. Laminate thicknesses are given in Table 3. Details for individual tests can be found in the SNL/MSU/DOE fatigue database [2].

The complex structured coupon geometry with ply drops is shown in Figure 6. Details of test development for complex coupon, and extensive static and fatigue data and simulation [10] results can be found in References 1, 5 and 10. Damage growth during static and fatigue tests is recorded by an automated camera system as well as visually.

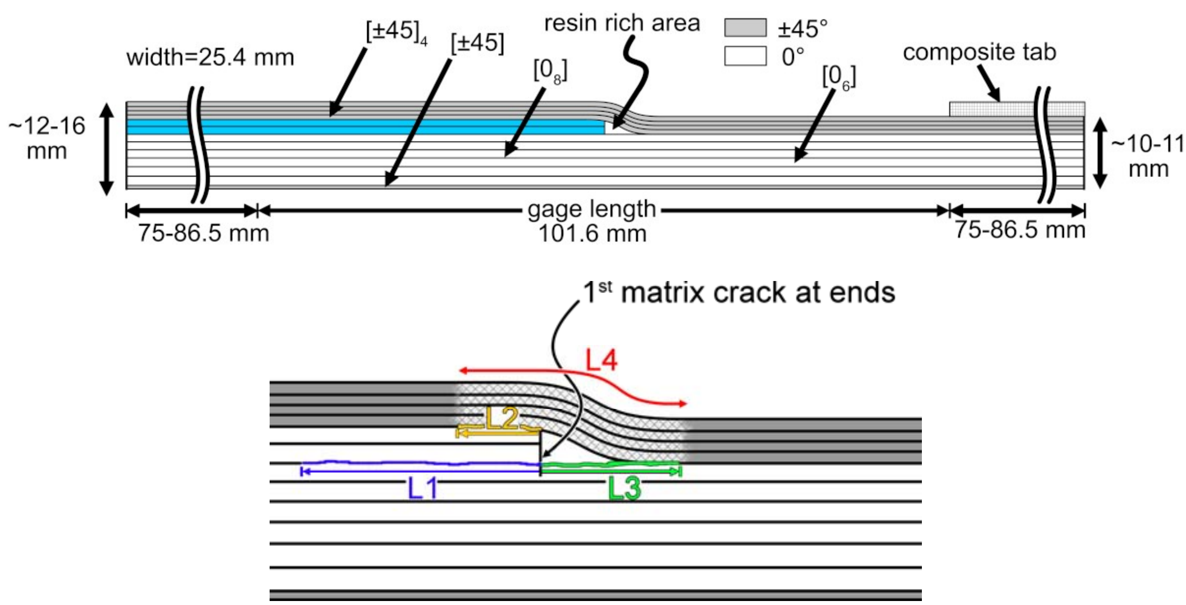

Figure 7. Test specimen and schematic of various damage components and extents in complex coupon [1,5,10].

III. Results and Discussion

A. Static Laminate Properties

Typical ply elastic constants and strengths for use in stress analysis are given in the database and contractor reports [1-3]. Typical static stress-strain curves are presented in Figures 8-10. Figure 8 compares the tensile and compressive stress-strain curves for a typical multidirectional laminate in the longitudinal direction, along with the component 0° and ±45° plies. The actual local fiber content of biax and mat layers in infused multidirectional laminates are well below that in the more closely packed uni-plies [1,3,11]. The multidirectional laminate stress-strain curves are dominated by the 0° plies in terms of modulus and failure strain. However, the nonlinear ±45^o (biax) plies contribute to the slight nonlinearity of the multidirectional laminate behavior in tension, as matrix cracking develops in these plies well before failure of the 0^o fibers (Figure 10). The process of matrix crack accumulation and material softening is typical of multidirectional laminates in tension [3].

Rate effects on static tensile strength have been widely reported for fiberglass [3]. Table 4 gives ultimate strengths at static test standard rates and typical fatigue test rates consistent with a frequency of a few Hz for selected laminates from Table 3. Static strengths are typically 15% higher at the higher rate for the multidirectional and biax fiberglass laminates.

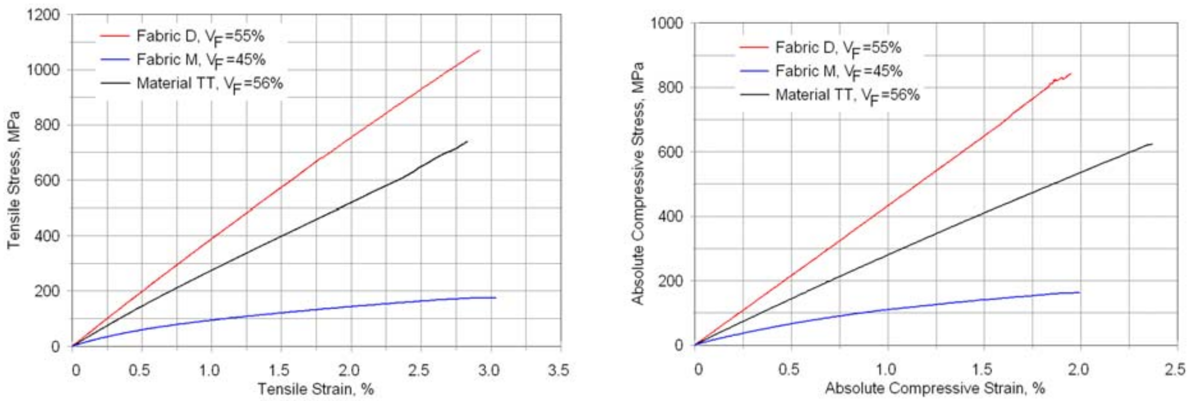

Figure 8. Tensile (left) and compressive stress-strain curves for laminate TT in the axial direction, with epoxy EP-1, comparison with component 0^o and ±45^o plies.

Laminates containing only biax (±45) fabric of three types have been tested with several resins [1]. While fabric construction and test direction have significant effects depending on the content of mat and the direction of strands used in fabric stitching (Table 2, Fabrics L, M, and O), the resin has limited effect for a particular fabric (Figure 10). Matrix cracking accumulates above where the tensile curves become nonlinear (see Fig. 9), and intensifies to include delamination prior to failure. In compression tests of various fabrics and multidirectional laminates, little matrix cracking was observed prior to failure, despite significant nonlinearity in the biax stress-strain curves [1]. Transverse loading of unidirectional laminates is an issue for unidirectional spar caps. Figure 11 indicates a significant resin effect, with the polyester cracking at a low strain, held together by the few transverse strands in the fabric backing at stresses above the knee where cracking develops (Table 2). The epoxy laminate is much stronger in the transverse direction, failing suddenly.

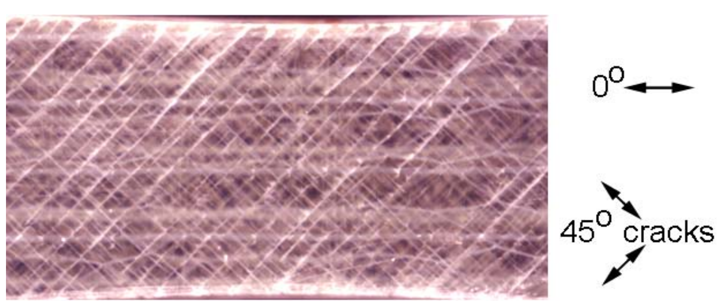

Figure 9. Cracking in ±45 plies of material QQ2 specimen prior to total failure [1].

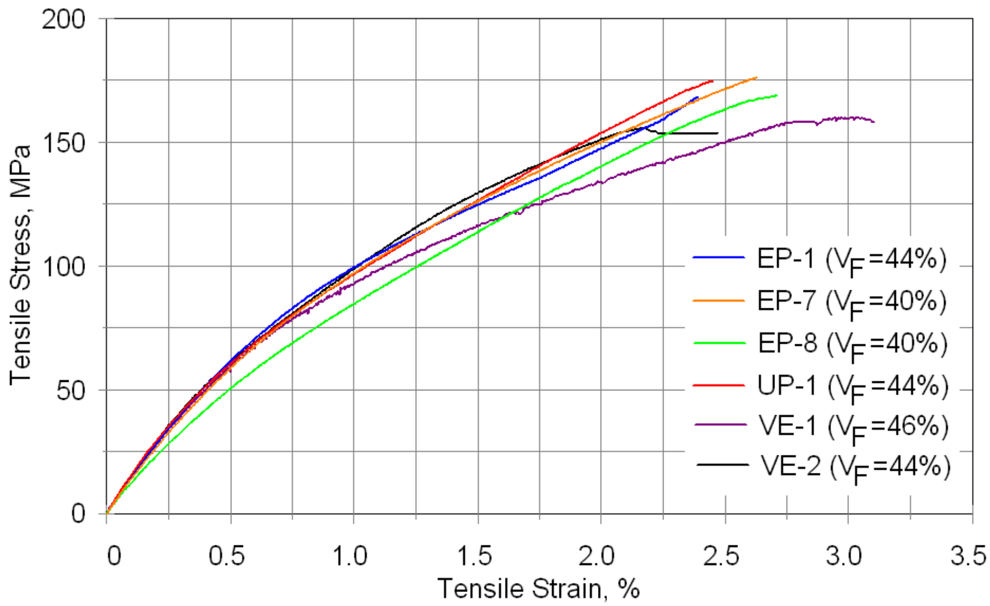

Figure 10. Comparison of tensile stress-strain curves for biax fabric M laminates with several resins at the indicated fiber contents, warp direction.

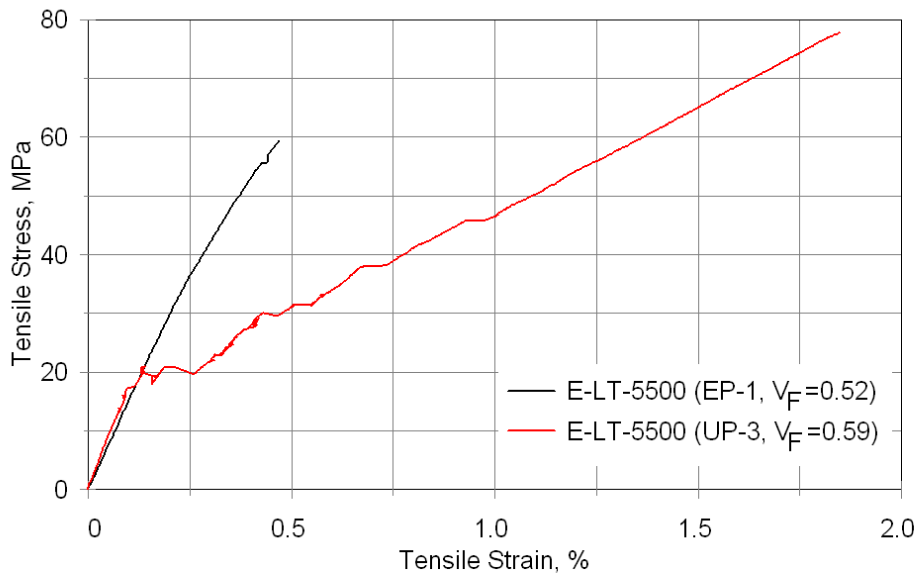

Figure 11. Transverse stress-strain curve comparison for Fabric D unidirectional laminates with resins epoxy EP-1 and polyester UP-1.

Table 4. Comparison of displacement rate effects on mean strengths (rates represent standard static and fatigue displacement rates in the axial direction).

Laminate	Tensile Strength, 13 mm/s (MPa)	Tensile Strength, 0.02 mm/s (MPa)	% Difference
TT-EP-1	812	700	-14
TT-UP-1	770	639	-17
QQ1	869	691	-21
DD16	632	549	-13
WS1	865	754	-13
TT-TPI-EP	837	732	-13
P2B	1546	1516	-2
DH	224	164	-27
DTR1	214	210	-2
45D	238	197	-17
45D2	207	167	-19
SWA	172	165	-4
WS1	223	157	-30

B. Fatigue of Standard Laminates

General Trends. Fatigue properties of a wide variety of laminates have now been reported [1-5], although comparisons are not available for all materials under controlled conditions. Data reported in recent publications have shown sensitivity to fiber type and strand alignment, resin, fabric construction, fiber content and process details. Data reported in this paper will explore several of these parameters under more controlled conditions than in the past. In particular, data for the effects of resin type and process details are significantly expanded.

The results in Figure 2 led to more detailed study of fabric and process effects. Processing by an improved blade analogue, resin infusion with one sided molds, resin distribution layers and vacuum bag, (designated Infusion, Figure 6) is compared with two sided hard molds (designated VARTM, Figure 5) where the laminate is forced to a desired thickness and fiber content. VARTM flattens any high spots in the perform stack even if the fiber content is near the natural condition for the dense fabrics at low pressure (Figure 4) [1]. The Infusion process produces a natural (but poorly controlled) fiber content at low (vacuum) pressure [1]. Figure 12 compares the tensile fatigue performance of the TT and TT1A multidirectional glass laminate structures (±45/0/±45/0/±45), with fabrics M, L and D, Table 3, with carefully controlled infusion conditions as well as VARTM data, for several epoxy resins. The data fall in a range similar to the material TT results (Fabric D) in Figure 2. The higher fiber content laminates tend to fall at the bottom of the band. Thus, the broad range of epoxy laminates in Figure 12 perform on a par with the material TT laminates in Figure 2. The data in Figure 12 include infused material QQ4, which had performed poorly when VARTM molded (Figures 1 and 2). However, when the QQ1 laminate in Figures 1 and 2 was infusion processed, the fatigue performance was unimproved compared with VARTM. Thus, with epoxy resins, some fabric structures and/or strands appear to produce more robust fatigue performance under a range of molding conditions, while others show consistently poor or else inconsistent performance. It should be noted that many of these results represent single moldings from single batches of fabric or resin; the strands vary, and are not identified for the fabric A, B or C unidirectional fabrics, and all biax fabrics in this series. As noted earlier (Table 2), Fabrics D, G, H and P contain PPG 2026 finish strands.

Figure 13 compares material TT-EP-1 from Figure 12 with three laminates having grouped 0^o plies and three different unidirectional fabrics, D, G and H. The tensile fatigue strains are very similar for these four laminates with the same epoxy resin and same PPG 2026 strand finish, also showing minimal effects of whether 0^o plies are separated by biax plies (TT-EP-1) or grouped in the mid-thickness with biax plies on the outside (TT2, TT5 and TT7).

By way of comparison to the epoxy laminates, three infused laminates were tested with different polyester resins, and fabrics which perform well with epoxy resins, as shown later. Figure 14 indicates very consistent tensile fatigue results for the three polyester laminates. As explored in the following, the strain levels for all of the polyester resin laminates fall significantly below those for the epoxy resin laminates in Figures 12 and 13.

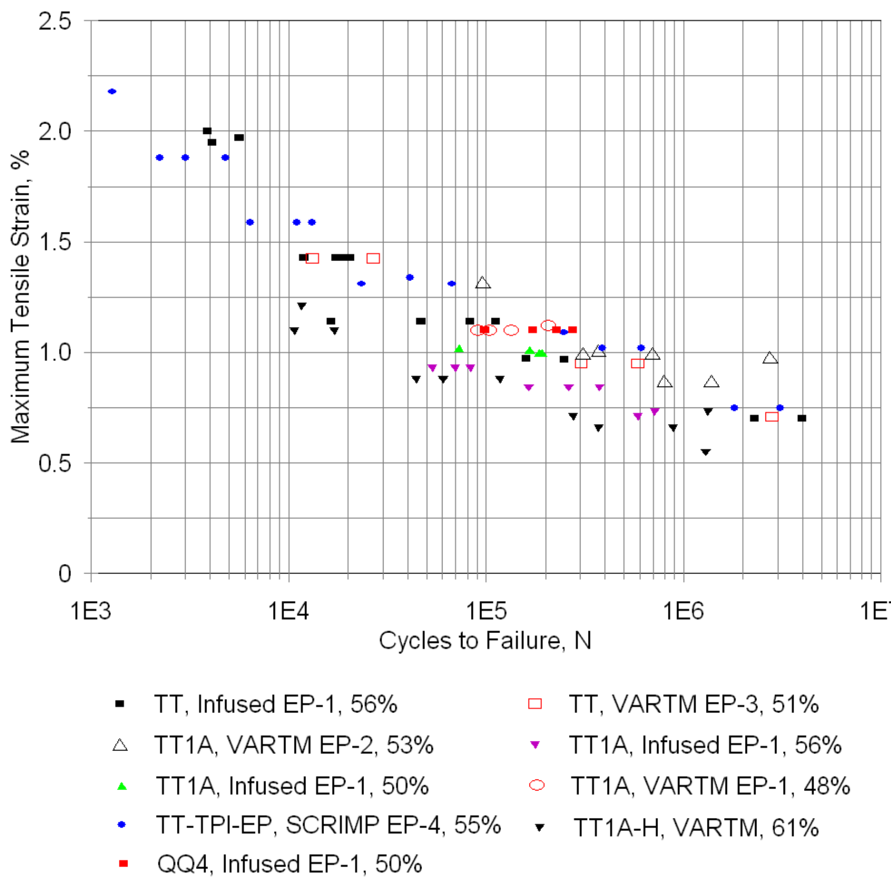

Figure 12. Tensile fatigue strain-cycles comparison for multidirectional laminates based on unidirectional fabrics C and D, different epoxy resins, batches, and processes.

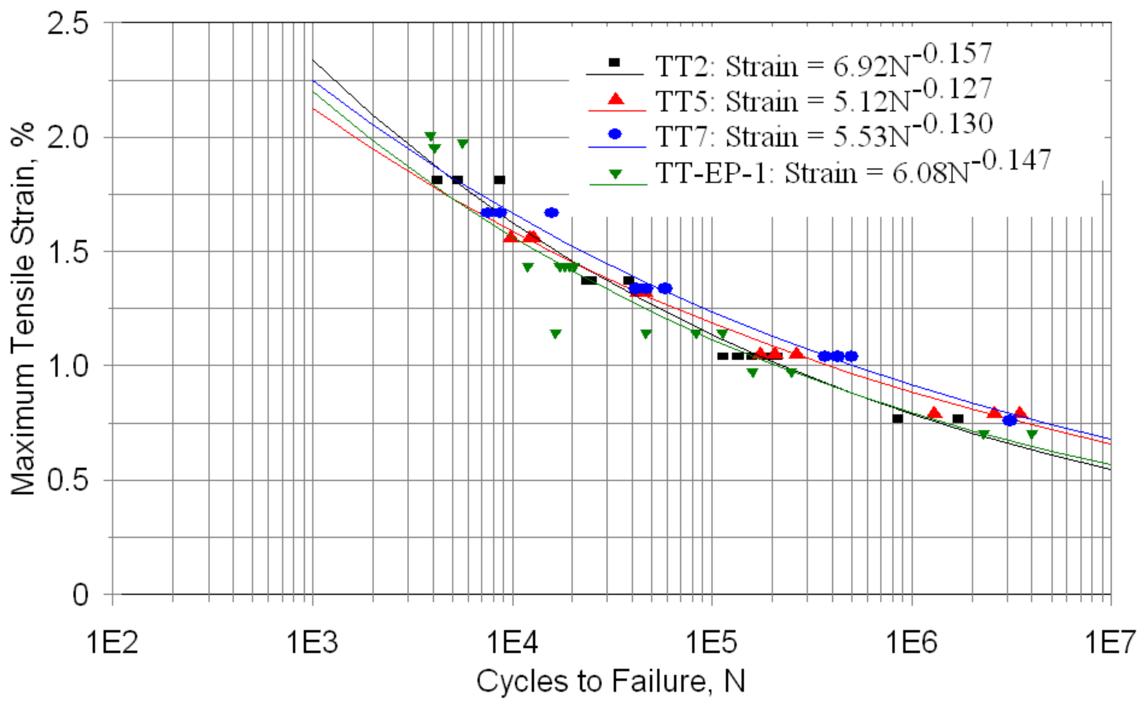

Figure 13. Comparison of epoxy resin EP-1 laminates with grouped 0° plies and three different unidirectional fabrics, with infused TT-EP-1 from Figure 12. (All unidirectional fabrics contain PPG Hybon ® 2026 sized strands.)

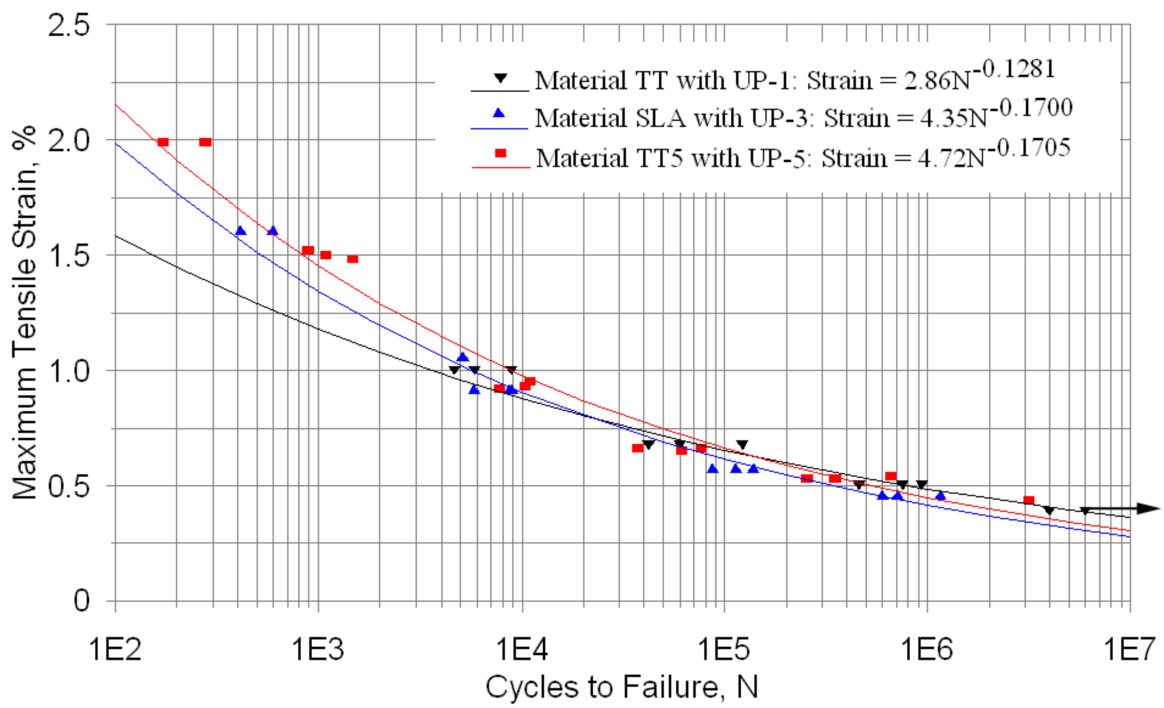

Figure 14. Tensile fatigue strain-cycles comparison for multidirectional laminates TT, SLA, and TT5, based on unidirectional fabrics D and G with three polyester resins.

Resin Comparisons. The results in Figures 13 and 14 indicate significant differences in general trends for epoxy and polyester resin laminates. Figure 15 gives a carefully controlled comparison using EP-1 and UP-1 (Table 1) and Fabrics D and M (Table 2) in the TT material configuration (Table 3). The differences are noteworthy; as illustrated on the strain plot, the million cycle strain for the polyester resin laminate falls 39% below the corresponding epoxy laminate value.

Alternative metrics for representing fatigue performance, in addition to million cycle strain, include fatigue exponents. Fatigue S-N data in the European Optimat program [9] are often presented as normalized stress, where the maximum stress is normalized by the ultimate tensile or compressive strength determined at the relatively slow rate of static test standards (Table 4). If the data fit includes only fatigue data, then the exponents on the normalized stress log-log plots such as Figure 16 are the same as those in Figure 15 for stress. If the fit includes static data, or is forced through the static strength at one cycle as in Figure 17, then the exponents are typically lower, around $B = -0.10$ ($n = -1/B = 10$, see Eq. 1). Actual exponents in this study, fit to fatigue data only (shown on the figures) vary considerably and sometimes do not correlate with the fatigue stress and strain differences between laminates. For example, for the strain curve fits in Figure 15, the epoxy resin laminate shows about 40% higher fatigue strains, while the exponent, B, suggests a less steep S-N curve for the polyester. The preferred approach for design is to obtain sufficient stress or strain fatigue results at five or six R-values, construct a constant life diagram, and predict blade lifetime using an acceptable cumulative damage law, as demonstrated in Reference 9. Since the tensile load containing R-values are most damaging for fiberglass, we prefer to compare laminates on the basis of the million cycle fatigue strain.

The bar graph in Figure 18 compares a range of polyester, vinyl ester and epoxy resin laminates on the basis of million cycle fatigue strain. Earlier data for different resin types at low fiber contents typical of hand lay-up showed nearly identical tensile fatigue sensitivity for polyester, vinyl ester and epoxy resins when VARTM and RTM processed with low density fabric A (Figure 3) [3]. However, recent reports [1,5,7] have indicated better performance with higher fiber content blade infusion fabrics for epoxy than for polyester, with vinyl esters intermediate, as shown on the right side of Figure 18. Million cycle strain values for all of the higher fiber content laminates fall significantly below corresponding values on the left for the lower fiber content laminates. These trends are also consistent with resin comparisons reported in Reference 10.

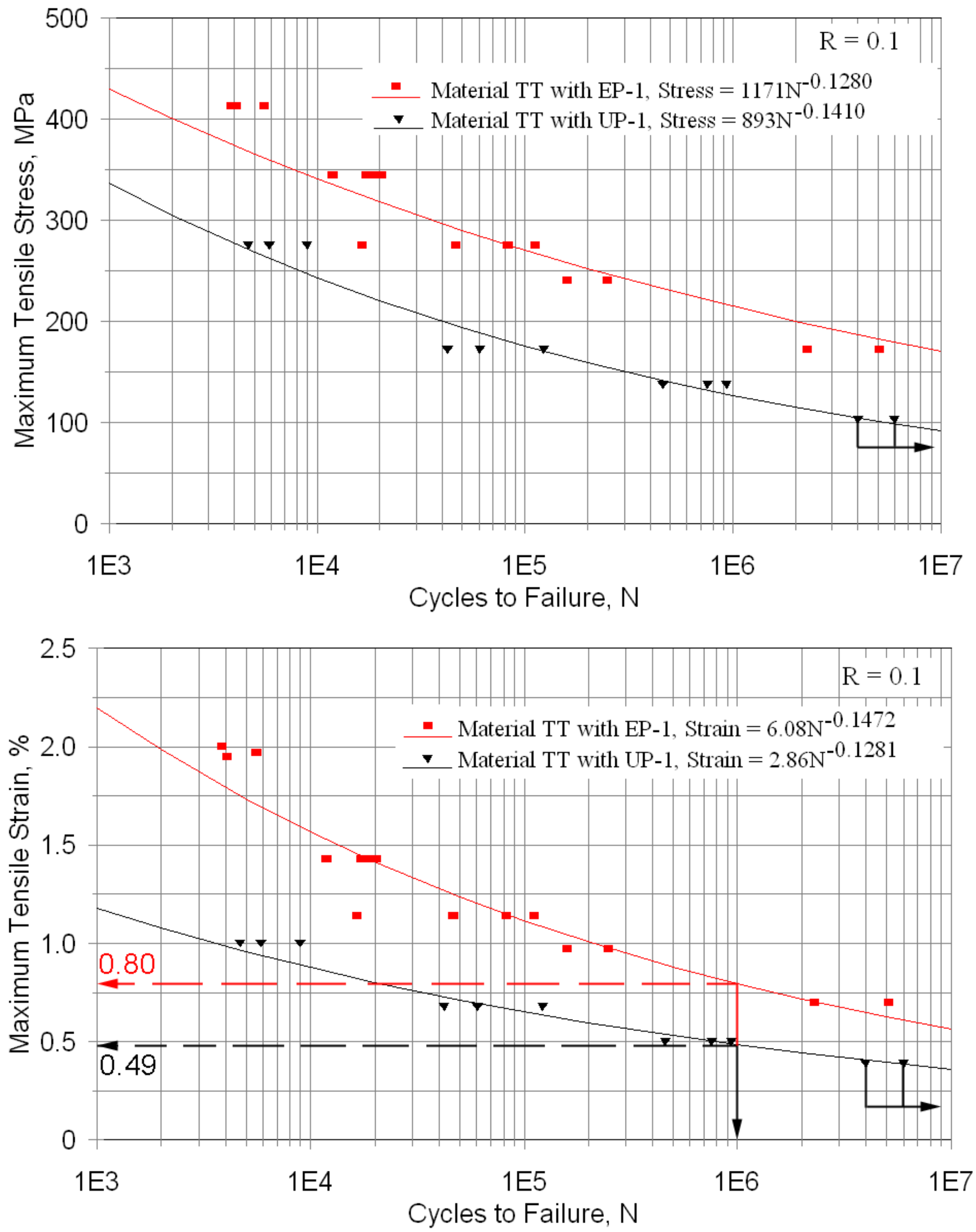

Figure 15. Stress (top) and strain vs. log cycles data for (±45/0/±45/0/±45) multidirectional infused laminates containing fabrics D and M, TT-EP-1 (epoxy, V_f = 52%), TT-UP-1 (polyester, V_f = 52%), R = 0.1.

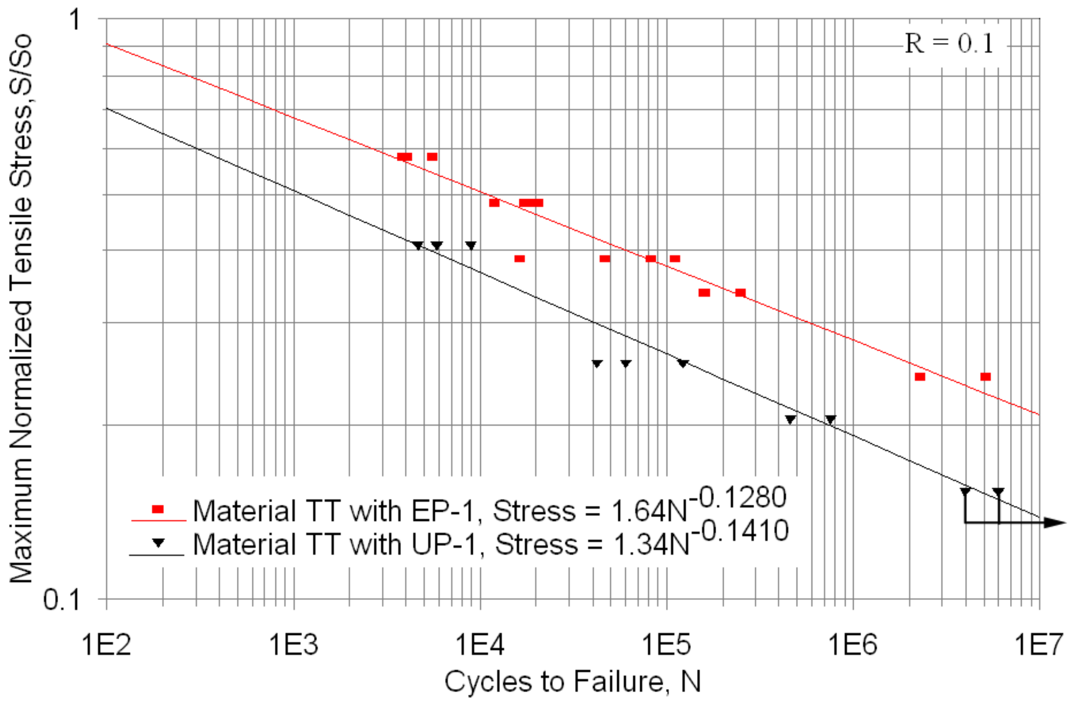

Figure 16. Log-log plot of stress data from Figure 15, normalized by static strength tested at 0.02 mm/s (Table 4).

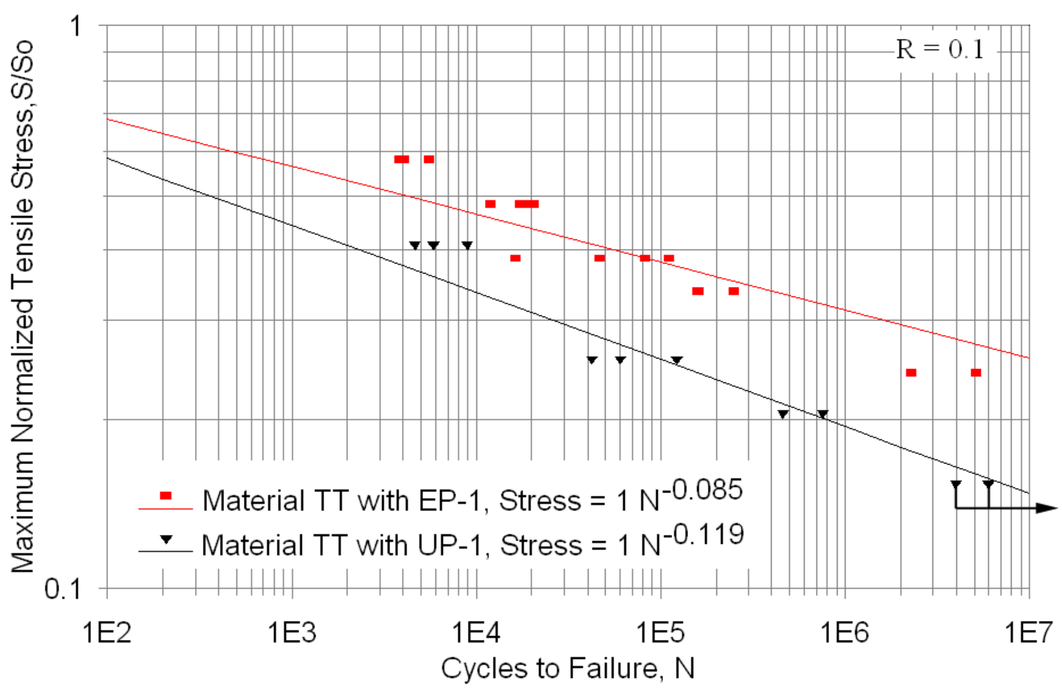

Figure 17. Figure 16 with curve fit forced through static strength (tested at 0.02 mm/s) at one cycle.

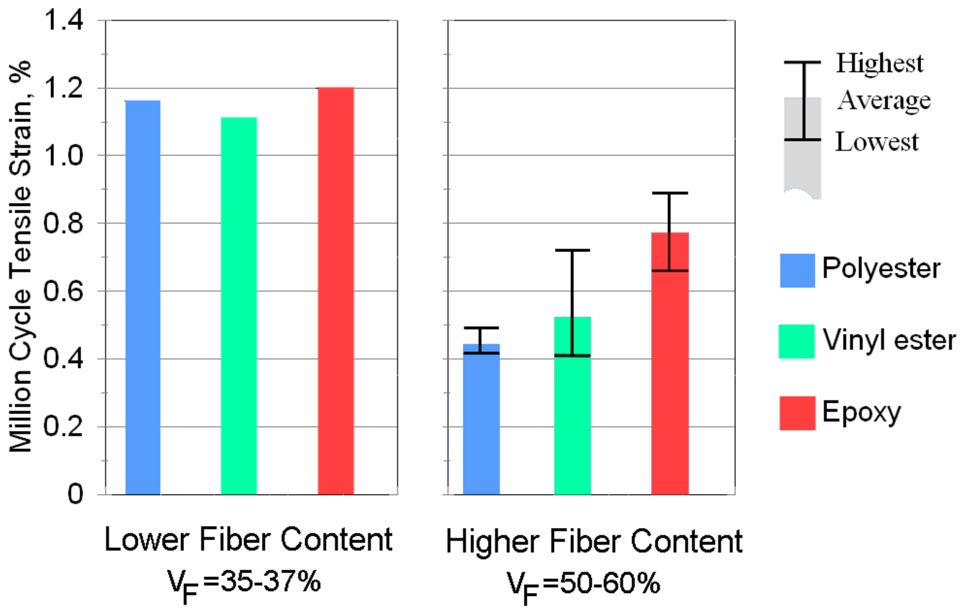

Figure 18. Comparison of polyester, vinyl ester and epoxy resin laminates at low (fabric A) and higher (fabrics D, G and H) fiber contents.

Origins of fabric and resin effects. The foregoing indicates that tensile fatigue resistance is significantly impacted by interactions between resin, fabric and fiber content; these are briefly explored in this section. Early data for low fiber content multidirectional laminates included in Figure 18 show no effect of the type of resin. These low density fabrics were also molded over a broad range of fiber contents with two-sided molds. The million cycle strain trend with fiber content is given in Figure 19 for multidirectional, unidirectional and biax laminates with polyester resin UP-2. The unidirectional laminate million cycle fatigue strain gradually decreases with increasing fiber content; the biax strain also decreases gradually with fiber content, but in a much lower strain range. For the multidirectional laminates, the million cycle strain follows the unidirectional strain at lower fiber content, then transitions to near the biax strain above about 45% fiber volume (plotted as DD-series in Figure 2, with Fabric A illustrated in Figure 3). The DD-series laminates are about 70% unidirectional material, 30% biax; at higher fiber contents the multidirectional laminates fail when the biax plies fail, at the relatively low fatigue strain capability of these biax materials. At low fiber contends the multidirectional laminates are able to withstand failure of the biax plies, eventually failing at the independent unidirectional ply strain condition.

The similar question is addressed for current high density fabrics in Figures 20-22. At typical infused multidirectional laminate fiber contents of 50-55% by volume, the epoxy data plotted in Figure 20 indicate that the multidirectional laminate fails a decade or more of cycles after the biax plies. The polyester resin data in Figure 20 indicate that the multidirectional laminates fail at about the same failure strain as the biax laminates. Figures 21 and 22, for a different set of fabrics and different polyester, compare the unidirectional laminate S-N results with the multidirectional laminates. Here, the multidirectional laminate strains follow only slightly above the unidirectional laminate strains. (The two polyesters in multidirectional laminates were shown to fail at nearly identical fatigue strains in Figure 18, and the two fabrics behaved similarly with the epoxy in Figure 12.) Thus, multidirectional laminates based on the dense infusion fabrics at 50-55% fiber volume content appear to fail in the same strain range as the unidirectional laminates for both resin types. The resin effect shown in Figure 12 derives from differences in the unidirectional ply fatigue resistance, which is matrix sensitive for these fabrics; these findings are consistent with those reported in Reference 10. For the polyester in Figure 20, the biax plies fail at about the same time as the unidirectional plies, and follow a very similar S-N trend. Improvements in the polyester and vinyl ester performance, to approach epoxy, may depend on fabric and strand finish developments more suited to those resins. The low fiber content results in Figure 18 demonstrate that these resins can perform on a par with epoxy under some conditions. It should also be remembered that some epoxy laminates have been found to perform more like the polyesters and vinyl esters with some fabrics like fabric B in material QQ1 (Figures 1 and 2).

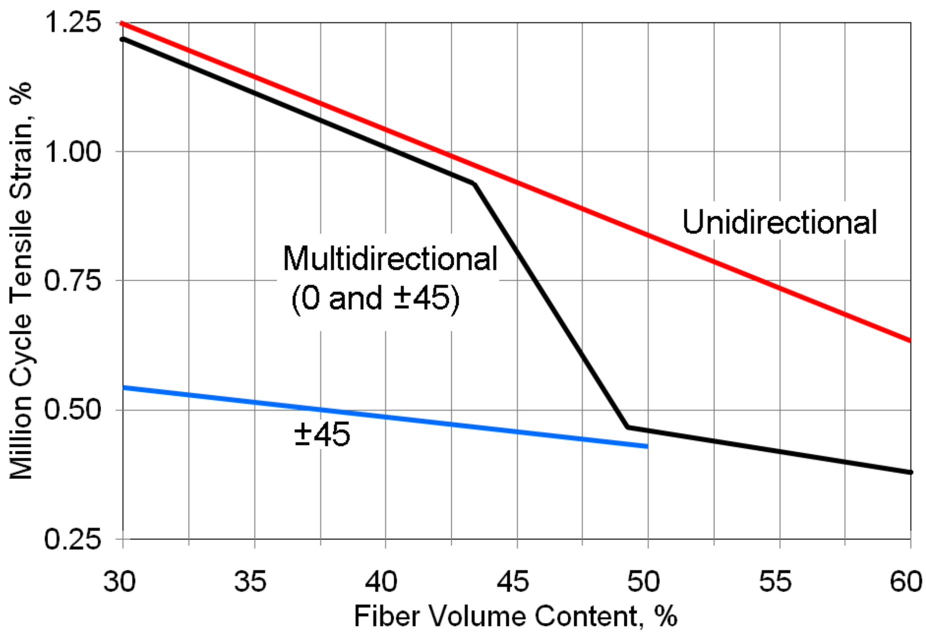

Figure 19. Fatigue trends vs. fiber content for unidirectional, multidirectional and biax laminates based on early [11] low density weft unidirectional fabrics D155 and D092, biax fabrics DB120 and DB240, with polyester resin UP-2.

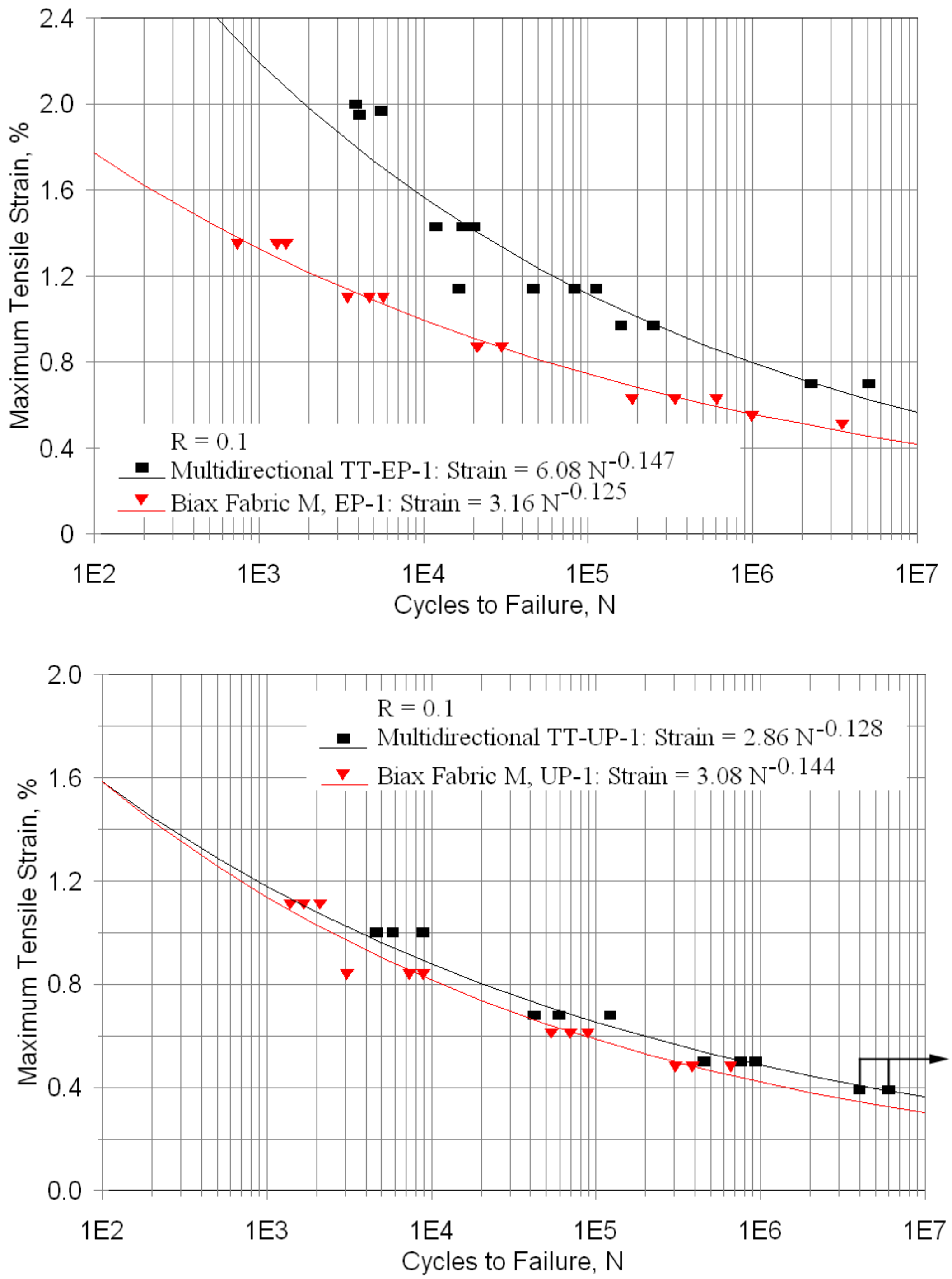

Figure 20. Comparison of multidirectional laminate fatigue strains with biax laminate fatigue strains for epoxy resin (top) and polyester resin (bottom).

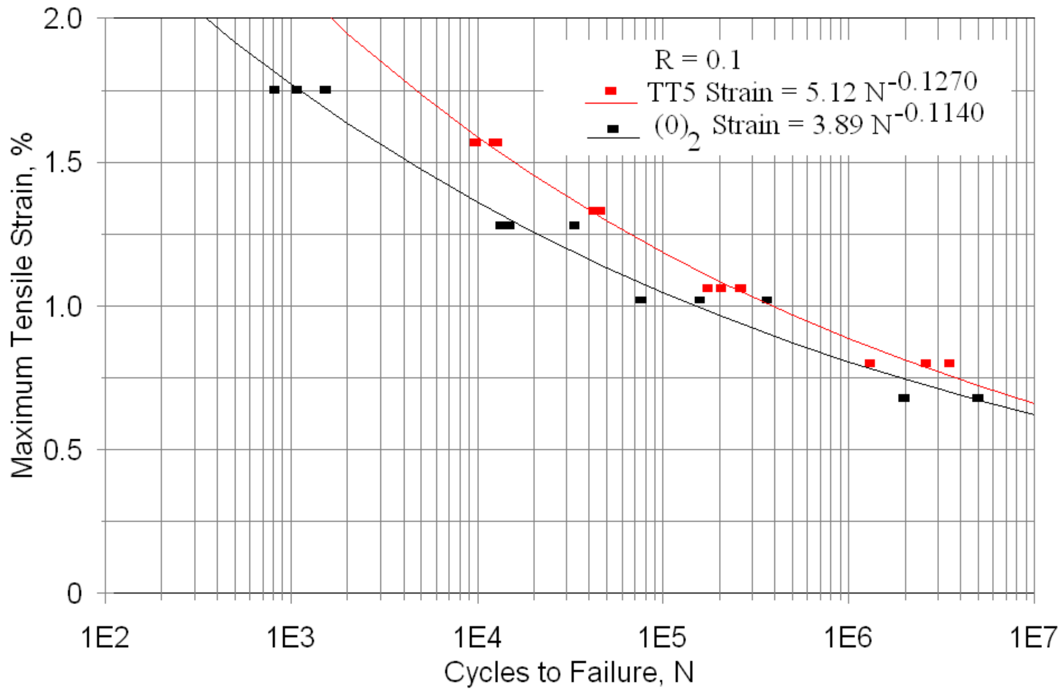

Figure 21. Comparison of epoxy multidirectional material TT5-EP-1 fatigue strains with unidirectional material UDH-EP-1 strains.

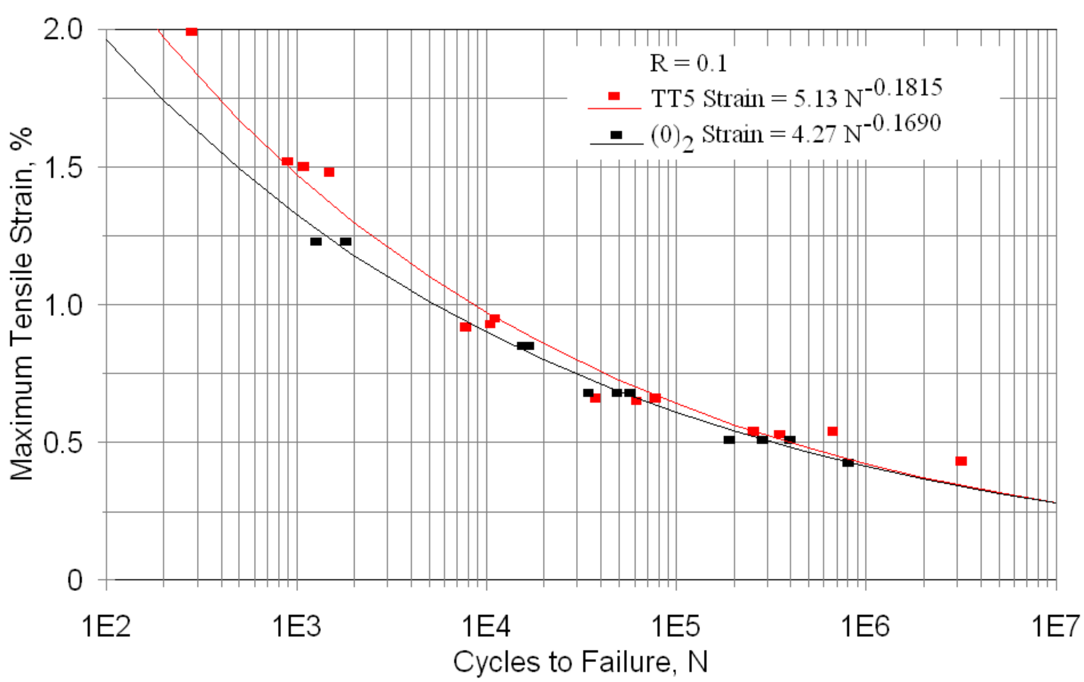

Figure 22. Comparison of polyester multidirectional material TT5-UP-1 fatigue strains with unidirectional material UDH-UP-1 strains.

Effect of Epoxy Cure Variations. Three cure conditions were explored for the epoxy EP-1 resin system in the multidirectional TT5-EP-1 laminate configuration. The results in Figure 23 indicate a moderate decrease in fatigue strains for curing at 35°C for 24 hrs followed by post-cure at 70°C for 12 hrs, relative to the standard cure used in this study of 20°C for 24 hrs and 80°C for 12 hrs. Subsequent post-cure of the 35/70 laminate for 4 hrs at 100°C produced the slight fatigue strain increase shown. As in most datasets, it should be emphasized that these results are for single moldings.

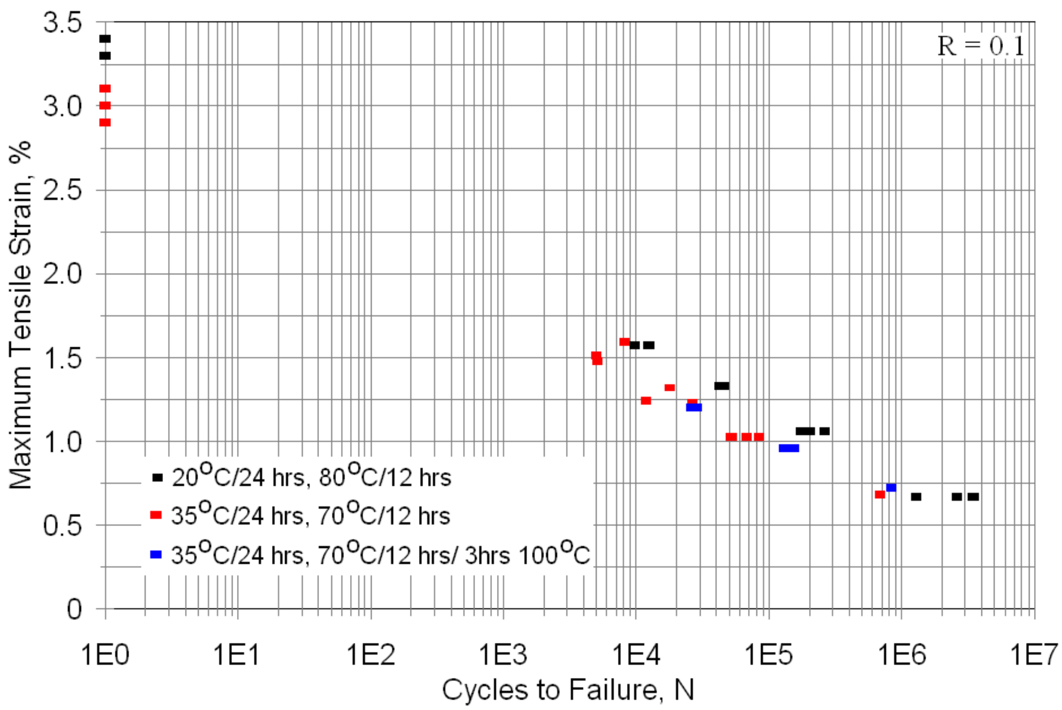

Figure 23. Effect of cure and post-cure conditions on epoxy EP-1, TT5 laminates.

Biax Fabric Laminates. The laminates consisting only of "biax" fabrics such as L and M in Table 1(d) have reduced mechanical properties in the axial direction, since most of the fibers are at ±45° (with the exception of small contents of mat or other 0° or 90° strands used in stitching the fabrics). These fabrics are common in skins and webs to provide shear and multidirectional properties, and to improve reinforcement handling and stability during assembly and infusion. Stress-strain curves for six resins (Table 1) with ±45 fabric M (which contains 30% mat) are given in Figure 5; the curves are significantly nonlinear in the stress range where fatigue tests were conducted, so fatigue data are given for both stress and initial cyclic strain in Figure 24. The most notable differences between resins are improved fatigue strains for toughened epoxy EP-8, and slightly reduced performance for the polyester UP-1.

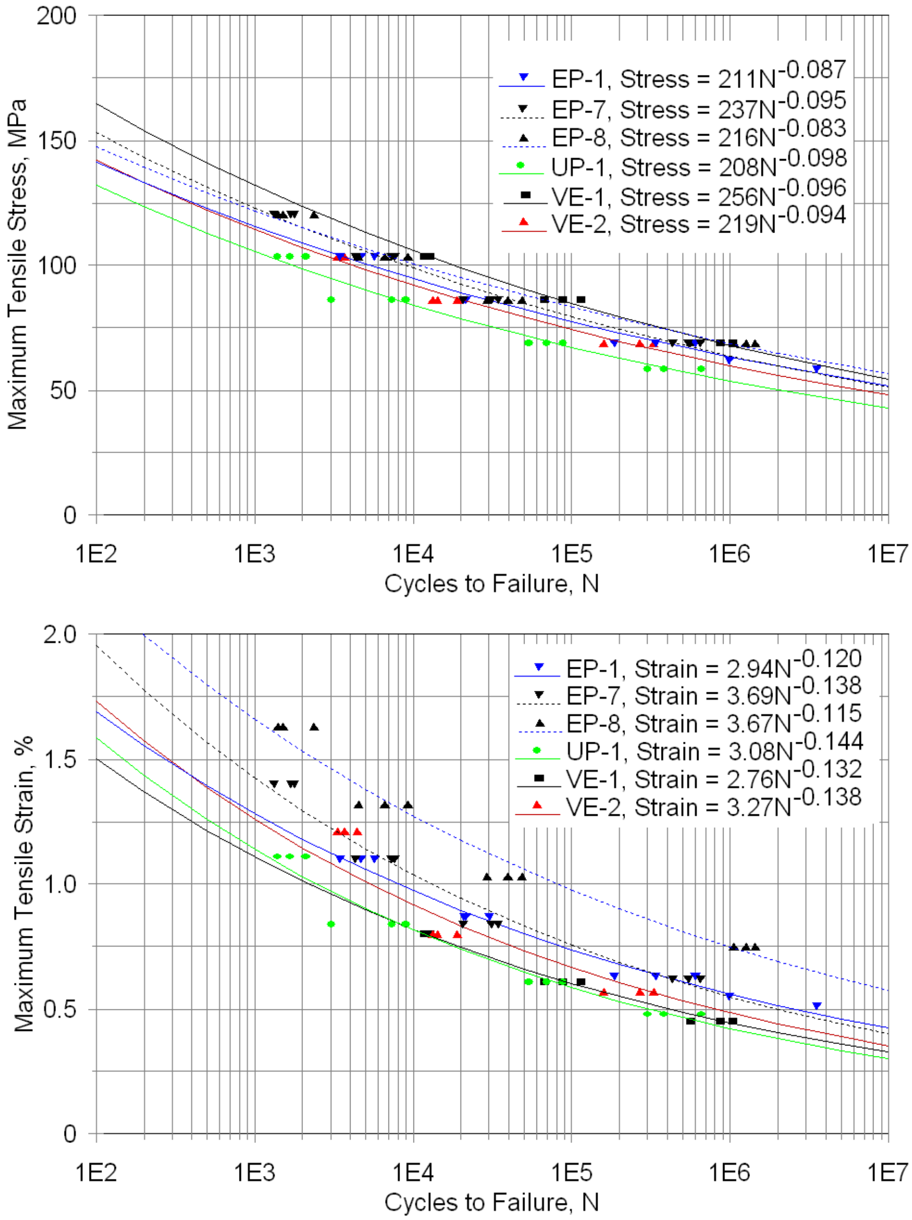

Figure 24. Stress (top) and initial strain (bottom) vs. log cycles data for fabric M, ±45 laminates with various resins (R = 0.1).

C. Test results for pDCPD resin system

The pDCPD resin system is a new type of thermoset with potential for wind turbine blades, having low density, low viscosity and very high toughness [12]. Test data are compared here with epoxy EP-1 resin laminates. The static multidirectional modulus, strength and ultimate strain properties listed in Table 5, and simulated shear stress-strain curve shown in Figure, generally indicate similar in-plane mechanical properties for the epoxy and pDCPD. The slightly higher fiber content for the pDCPD laminates is reflected in the static properties; the higher simulated shear stress-strain curve (ASTM D3518) appears to reflect greater matrix cracking resistance in the pDCPD.

The most notable difference between the epoxies and the pDCPD in Table 5 is the much higher delamination resistance, G_{Ic}, for the pDCPD. The G_{Ic} value of 1560 J/m^2 is in the range of very highly toughened epoxies like F185 [13] and high performance thermoplastics like PEEK (APC2) [13,14]. G_{IIc} values for the un-toughened epoxies are generally high, reflecting the complex cracking mechanism involved in crack advance [14]. Tough resins like PEEK [14] and pDCPD deform in a ductile manner in both modes, and have similar high toughness values in modes I and II.

The tensile fatigue performance of the multidirectional pDCPD laminates is similar to that for the various epoxy resins using the highest performance uni-fabric D, as shown in Figure 26. The pDCPD data fall near or above those for the epoxy laminates having similarly high fiber contents. The compressive fatigue results given in Figure 27 show slightly improved compressive fatigue resistance for the pDCPD compared to the epoxy.

Table 5. Average Static Properties for Infused Multidirectional Laminates, and G_{Ic} and G_{IIc} for Unidirectional Laminates

Resin	**EP-1 epoxy (TT1A laminate)**	**pDCPD (TT1A-pDCPD)**
Thickness, mm	4.24	4.07
V_f, %	55.6	60.1
Elastic Modulus E, GPa	29.7	30.3
Tensile Strength, MPa	910	928
Ult. Tensile Strain, %	3.2	3.1
Compressive Strength, MPa	-670	-632
Ult. Compressive Strain, %	-2.2	-2.1
G_{Ic}, J/m^{2*}	330	1560
G_{IIc}, J/m^{2*}	3446	2728

*Unidirectional fabric D laminate ($0_2/0_2$), 0/0 interface, EP-1 V_f = 60%, and pDCPD V_f = 64%.

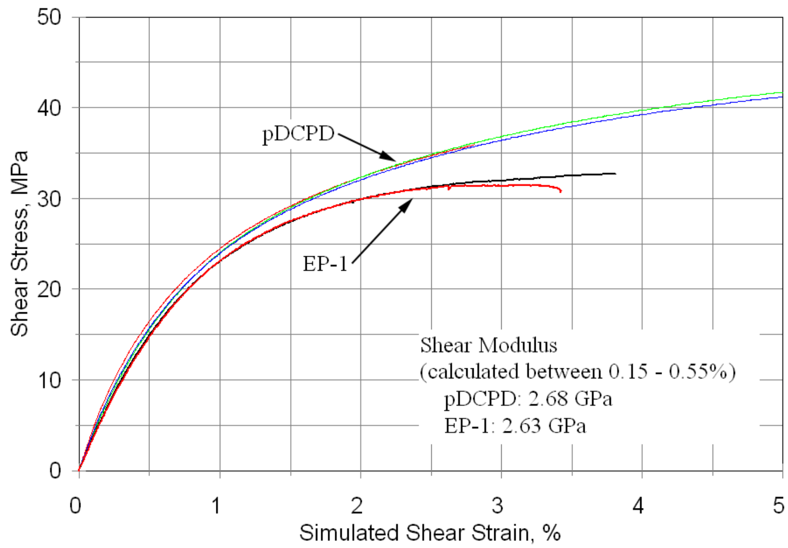

Figure 25. Simulated Shear Stress-Strain Curves, ±45 Fabric D.

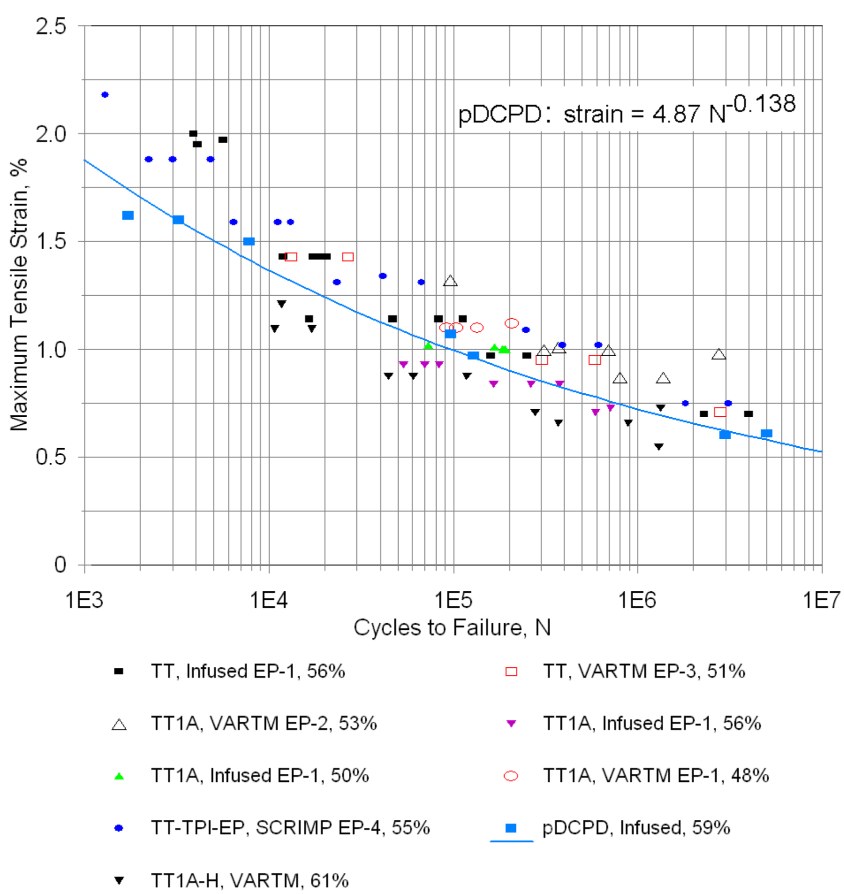

Figure 26. Tensile Fatigue Data and Trend Line for pDCPD Multidirectional Laminate Compared with Various Epoxy Data from Figure 12, R = 0.1; All Laminates Use the Same Uni-fabric D.

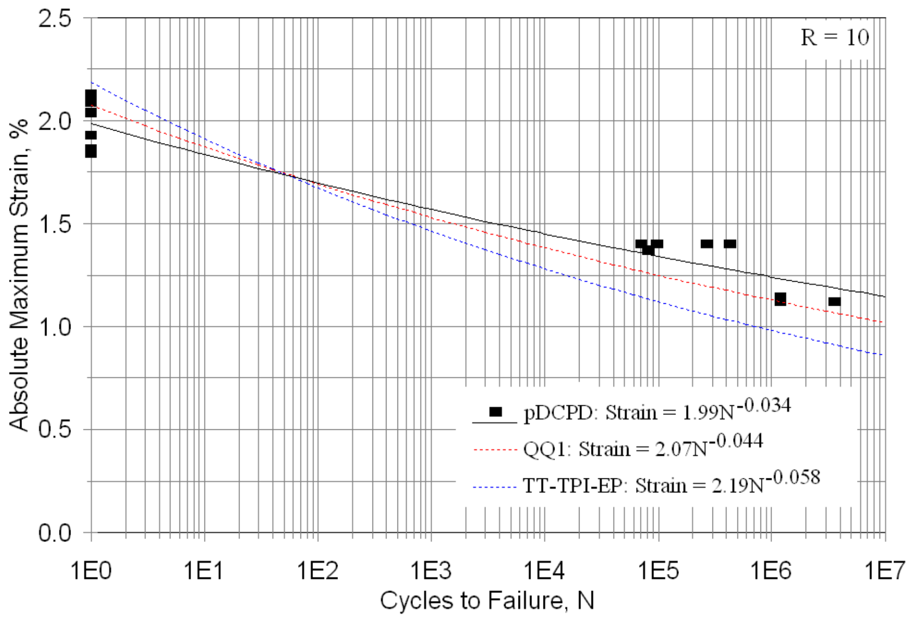

Figure 27. Compression Fatigue Data and Trend Lines for TT1A- pDCPD Multidirectional Laminate Compared with Trend Lines for Epoxy Laminates QQ1 and TT-TPI-EP from Reference 1, R = 10.

D. Complex Structured Coupon

The concept in this study is based on a new complex structured coupon test for infused laminates, representative of thickness tapered blade structure with ply drops [1,5,8]. The test allows comparison of different resin types, fabrics and ply drop geometric details, under tension, compression and reversed loading, in terms of both damage growth characteristics and strain knockdowns.

The complex structured coupon provides a basis for comparing infusion blade material and lay-up parameters for a case which is more representative of real blade structure than are plain laminate tests. The sequence of damage initiation and growth illustrated in Figure 7 depends on both in-plane properties of the fabric layers and interlaminar properties, the latter dominated by the resin. The test coupon geometry, designed by FEA, shows minimal effects of non-symmetry, which allows for increased thickness coupons more representative of blades. Figure 29 shows a typical damage progression for vinyl ester VE-1. Initial results from static and fatigue tests again indicated improved performance epoxy relative to vinyl ester or polyester; a toughened vinyl ester performed on a par with epoxy, Figures 30 and 31. Figures 32 and 33 indicate improved performance for pDCPD relative to epoxy EP-1 in static loading and higher cycle fatigue, the latter shown for reversed loading. Test results for various resins with the complex coupon are consistent with delamination data in Table 6 for pure mode I and mode II tests [1,11]. Simulations of the static response, featuring a mixed mode delamination criterion and softening of the biax plies, are presented in Reference 8. The data for different ply drop geometries are reduced to a strain based comparison useful as design knockdowns, Figure 34. For the two ply drop geometry, about 2.6 mm total thickness drop, the polyester fatigue strain is about 24 % below the epoxy value in the 10^5 cycle range.

Table 6. Pure mode delamination test results with unidirectional laminates, 0_{90} fabric D. (Numbers in parenthesis are standard deviations for 3-5 tests.)

Resin	0-0 Interface ($0_{90}/{}_{90}0//0_{90}/{}_{90}0$)				90-90 Interface (${}_{90}0/0_{90}//{}_{90}0/0_{90}$)			
	V_F, %	Initial G_{IC}, J/m²	V_F, %	Initial G_{IIC}, J/m²	V_F, %	Initial G_{IC}, J/m²	V_F, %	Initial G_{IIC}, J/m²
EP-1	60	303 (40)	60	3446 (201)	62	321 (38)	61	1887 (97)
UP-1	60	166 (17)	60	1662 (200)	62	175 (27)	62	928 (353)
VE-1	64	252 (24)	63	2592 (130)	64	223 (13)	63	1653 (124)
VE-2	61	433 (53)	61	2998 (313)	61	272 (33)	61	1689 (349)
pDCPD	64	1560(241)	64	2728 (305)	---	---	---	---

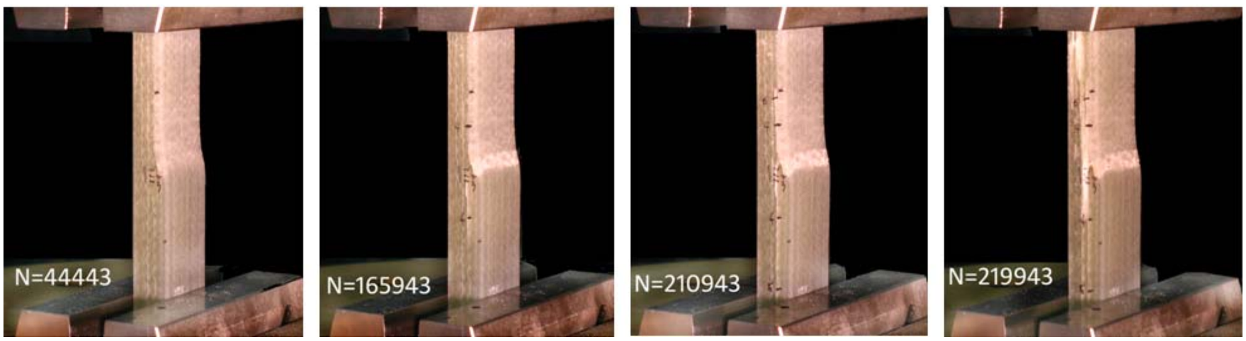

Figure 29. Images of damage in complex coupon with VE-1 resin, two ply drops, maximum load 44.5 kN, R = 0.1, at four cycle levels, N = 44443, 165943, 210943, 219943 [5].

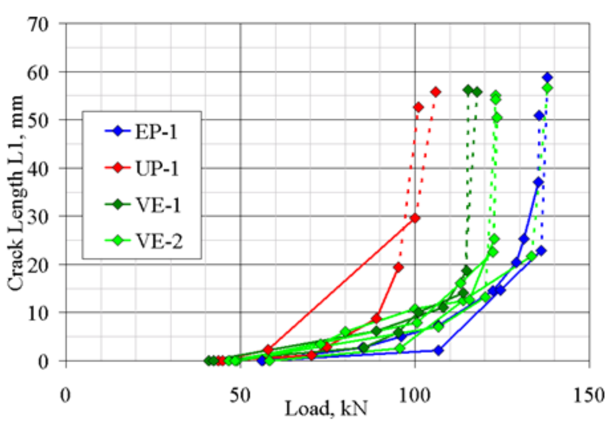

Figure 30. Static ply drop results for delamination growth, L1, vs. load, various resins, two plies dropped, fabrics M and D.

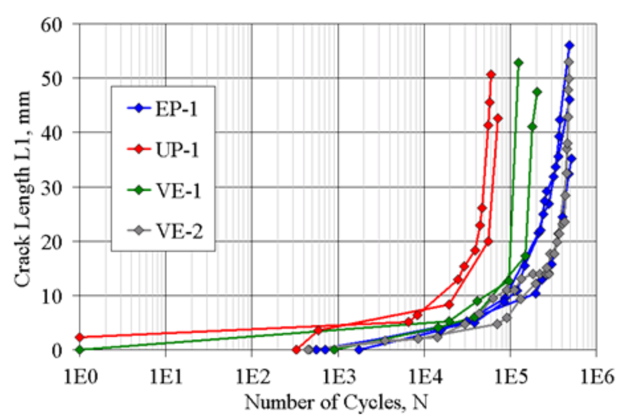

Figure 31. Fatigue test results with R=0.1 at 44.5 kN maximum load for various resins with two plies dropped, fabrics M and D.

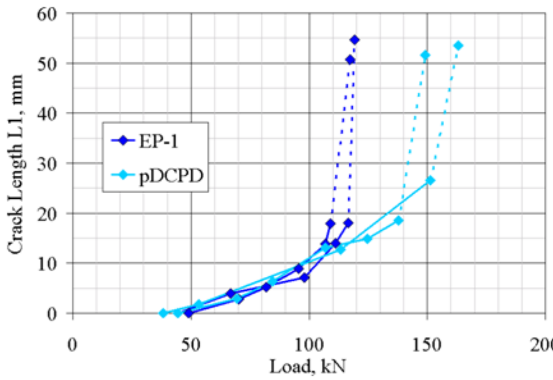

Figure 32. Comparison of epoxy and pDCPD under static loading, two plies dropped, fabrics L and D

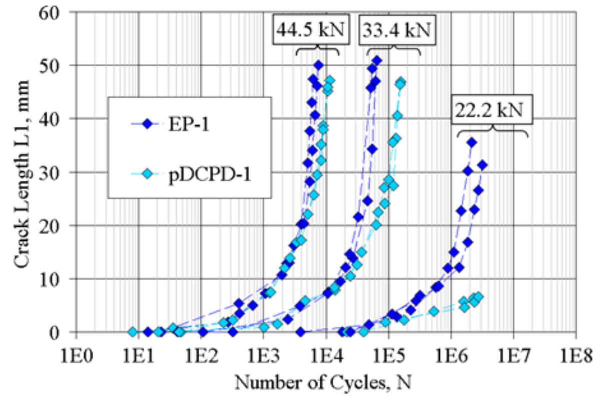

Figure. 33 Epoxy and pDCPD under reversed loading R=-1, at various maximum load levels, fabrics L and D

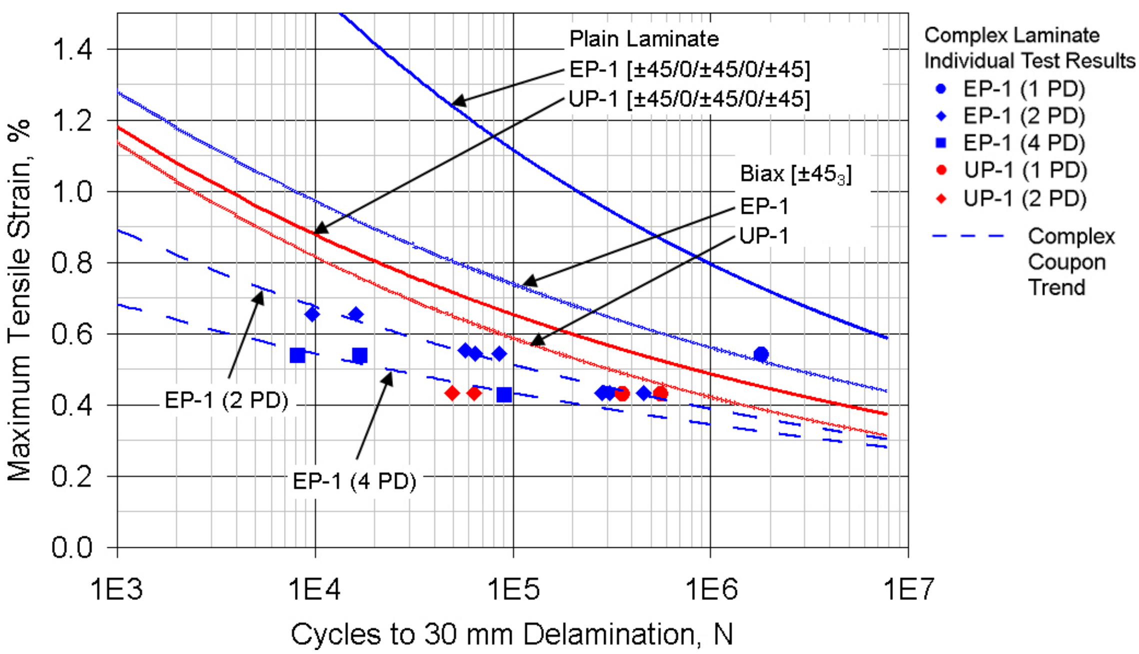

Figure 34. Complex structured coupon results for average thin-side strain, for 1, 2 and 4 ply drops (PD) at the same position for Epoxy EP-1 and Polyester UP-1, compared with corresponding plain (no ply drop) multidirectional and biax laminate trend lines, R = 0.1.

IV. Conclusions

The fatigue resistance of infused blade laminates shows a strong sensitivity to resin, fabric and fiber content interactions. Polyester resins at typical infusion fiber contents of 50-60% show fatigue strains 30-40% below those for epoxies, with vinyl esters intermediate. Some fabrics perform in the polyester range for epoxies as well. Multidirectional laminate fatigue strains than do unidirectional laminates; with epoxy resins, multidirectional laminates survive for a decade or more of cycles after biax failure, before total failure. Biax and unidirectional plies fail at similar strains for the polyester resin laminates tested.

The pDCPD resin has low density and viscosity and high toughness. Standard laminate data show similar static strength and modulus, with greatly increased interlaminar toughness, G_{Ic}, relative to the baseline epoxy. The tensile fatigue resistance is similar to that for epoxy laminates with similar fiber content, while the compressive fatigue resistance is slightly improved over epoxy.

Performance in the complex structured coupon with ply drops is strongly resin dependent, with an ordering from lowest to highest performance of: polyester, vinyl ester and epoxy, with a toughened vinyl ester performing similarly to the epoxy. The pDCPD resin performed better than the epoxy in static and higher cycle fatigue tests.

Acknowledgements

This research was supported by Sandia National Laboratories, Tom Ashwill, technical manager. The support and encouragement of the many industry materials suppliers is greatly appreciated.

References

1. Mandell, J. F., Samborsky, D.D., Agastra, P., Sears, A.T. and Wilson, T.J., “Analysis of SNL/MSU/DOE Fatigue Database Trends for Wind Turbine Blade Materials,” Sandia Contractor Report, To Be Published (draft available on www.coe.montana.edu/composites/).
2. Mandell, J.F. and Samborsky, D.D., “DOE/MSU Fatigue of Composite Materials Database, 2009 update (www.sandia.gov/wind/other/973002upd0309.pdf).
3. J.F. Mandell, D.D. Samborsky, and D.S. Cairns, “Fatigue of Composite Materials and Substructures for Wind Turbine Blade,” Contractor Report SAND2002-0771, Sandia National Laboratories, Albuquerque, NM, (2002).
4. Samborsky, D.D., Wilson, T.J. and Mandell, J.F., J. Sol. Energy Eng., 2009, 131, paper 011006.
5. Agastra, P., Samborsky, D.D. and Mandell, J.F., “Fatigue Resistance of Fiberglass Laminates at Thick Material Transitions,” paper AIAA-2009-2411, AIAA SDM Conf., Palm Springs, 2009.
6. Griffin, D., “Blade System Design Study Part II: Final Project Report (GEC),” Contractor Report SAND2009-0686, Sandia National Laboratories, Albuquerque, NM (2009).

7. Mandell, J.F., Samborsky, D.D. and Agastra, P., Proc. SAMPE 2008, Long Beach, CA, paper L238, 2008.
8. Agastra, P. and Mandell, J.F., ‘Testing and Simulation of Blade Damage Growth at Ply Drops in Wind Turbine Blade Materials,” SAMPE 2010, Seattle, paper 398.
9. Nijssen, R.P.L., "Fatigue Life Prediction and Strength Degradation of Wind Turbine Rotor Blade Composites," Contractor Report SAND2006-7810P, Sandia National Laboratories, Albuquerque, NM, 2006.
10. Nijssen, R.P.L., Westphal, T., Stames, E. and Sari, J., “Fatigue of Wind Turbine Rotor Blade Composites and Subcomponents,” SAMPE SEICO, Paris, April, 2010.
11. Mandell, J.F. and Samborsky, D.D. "DOE/MSU Composite Material Fatigue Database: Test Methods, Materials, and Analysis," Contractor Report SAND97-3002, Sandia National Laboratories, Albuquerque, NM (1997).
12. Egecombe, B. D., Cruce, C., Stephen, T, McCarthy, T., Mandell, J. F., Samborsky, D. D., Agastra, P. and Wetzel, K. K. ,“Effects of a new, high-toughness infusion resin on the fatigue performance and defect-tolerance of glass composite laminates,” *AWEA Windpower conference*, Dallas, May 2010
13. Russell, A.J. and Street, K.N., “The effect of matrix toughness on delamination: static and fatigue fracture under Mode II shear loading of graphite fiber composites,” Toughened Composites, ASTM STP 937, N. J. Johnston, Ed., American Society for Testing and Materials, Phil., 1987, pp. 275-294.
14. Johnson, W.S. and Mangalgiri, P.D., “Influence of the resin on interlaminar mixed mode fracture,” Toughened Composites, ASTM STP 937, N. J. Johnston, Ed., American Society for Testing and Materials, Phil., 1987, pp. 295-315.